JCTC Journal of Chemical Theory and Computation

Radical-Induced Damage in 3′dTMP − Insights into a Mechanism for DNA Strand Cleavage†

Ru bo Zhang,‡,§ Feng xin Gao,‡ and Leif A. Eriksson*,§

The Institute for Chemical Physics and School of Science, Beijing Institute of Technology, Beijing 100081, China, and Department of Natural Sciences and Örebro Life Science Center, Örebro University, 701 82 Örebro, Sweden

Received December 13, 2006

Abstract: DNA strand scission and base release in 3′dTMP, induced by H and OH radical addition to thymine, is studied at the DFT B3LYP/6-31+G(d,p) level in the gas phase and in solution. In particular the mechanism of H atom transfer subsequent to radical formation, from C2′ on the sugar to the C6 site on the base, is explored. Bulk solvation is found to lower the barrier by up to 5 kcal mol^{-1} and the reaction energy by up to 12 kcal mol^{-1} for the hydroxyl radical adducts. The strengths of the N1−C1′(N1-glycosidic bond) and C3′−O(P) bonds are calculated, showing that homolytic bond breaking processes are largely favored in both cases. The barrier for C3′−O(P) bond rupture is approximately 18.2 kcal mol^{-1}, and its breakage is preferred by 10−15 kcal mol^{-1} over that of N1-glycosidic bond cleavage in both the gas phase and solvents, which is consistent with the changes in C3′−O(P) and N1−C1′ bond lengths during the H transfer reactions. Mulliken spin densities, NPA charges, and vertical electron affinities are calculated to clarify the reactive properties of the intramolecular H-transfer radicals.

1. Introduction

Radical attack on DNA is one of the main reasons for DNA damage.[1] Electron paramagnetic resonance (EPR) spectroscopy in conjunction with spin-trapping carried out in aqueous solution has shown that H, OH, and alkoxyl radicals can attack the C5−C6 double bond of the pyrimidine base moieties via addition or the sugar moiety via hydrogen abstraction, in nucleosides, nucleotides, and DNA.[2−4] Thiyl radical attack on the C6-position of pyrimidine nucleosides has also been reported.[5] The chemical behavior of phenyl radicals toward DNA and its components has been extensively investigated.[6] Much theoretical work has been devoted to unveil the effects and mechanisms of radiation in DNA lesion formation. In the case of thymidine, the hydroxyl radical may either add to the C5═C6 double bond or abstract a hydrogen atom from the C5 methyl group, with addition to C5 being the major pathway.[7] For H atom addition, formation of the 5,6-dihydro-6-thymyl radical is preferred over the corresponding 5-thymyl radical, although the relative energy difference between the two products is only 3.1 kcal/mol.[8] A competing set of reactions is posed by H atom abstraction by the OH radical from the sugar moiety. These depend on the C−H bond strength and lead to alteration of the sugar moiety and subsequent rearrangements that in turn have been suggested to generate base release or strand break.[9,10]

It is generally accepted that nucleobase-radical adducts contribute to strand break.[11−13] The exact mechanism is, however, uncertain to date. Electron spin resonance (ESR) results have indicated this to be a slow process,[14] with the rate-limiting step suggested to involve intra- or internucleotide hydrogen atom abstraction from a sugar group (paths A and C, shown schematically in Scheme 1).[15] This process has also been proposed to proceed by way of initial protonation of the radical adduct, followed by dehydration to form the radical cation, intramolecular H-transfer, and strand scission (path B of Scheme 1).[16] The mechanism involving intranucleotide hydrogen atom abstraction as well as protonation/dehydration pathway has been

† Dedicated to Dennis R. Salahub on the occasion of his 60th birthday.

* Corresponding author e-mail: leif.eriksson@nat.oru.se.

‡ Beijing Institute of Technology.

§ Örebro University.

10.1021/ct6003593 CCC: $37.00
Published on Web 02/23/2007

Scheme 1

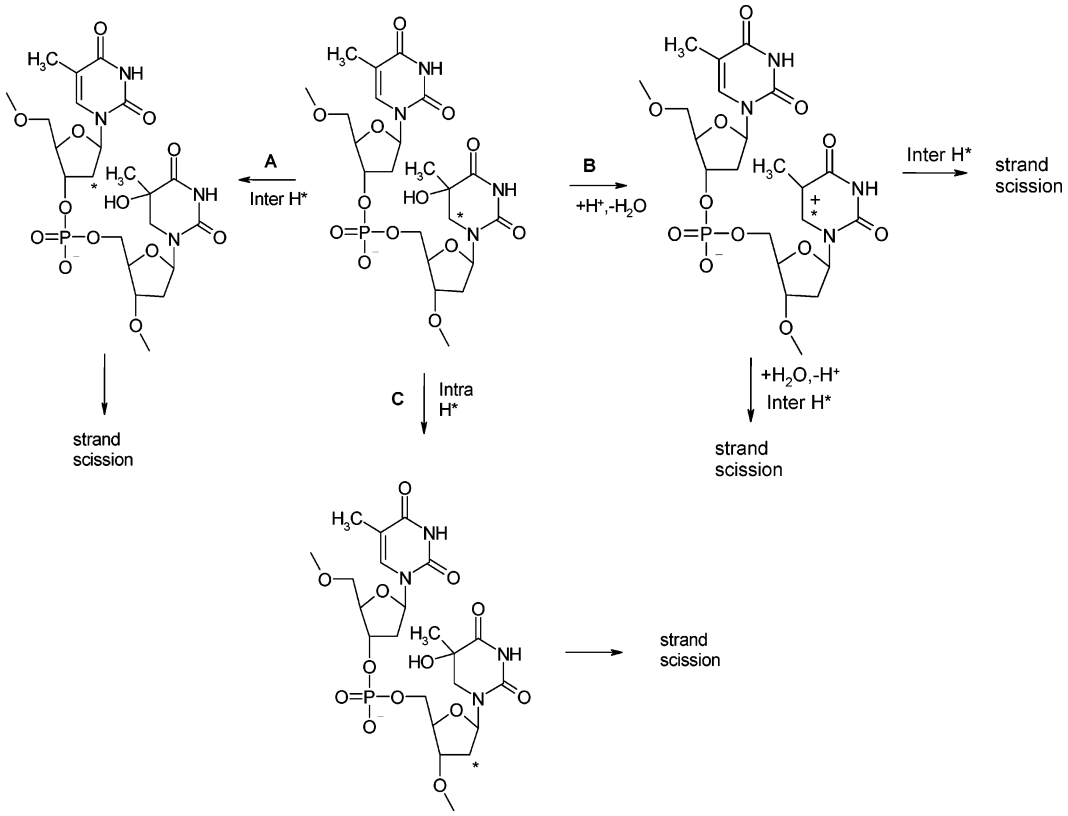

proposed to be less important in the biopolymer, due to the stability of the nucleobase-radical adduct.[17] It is evident that the above processes often are quenched in the presence of oxygen molecules although they have been reported to occur in hypoxic cells.[11]

The OH and H radical adducts of the pyrimidines at either C5 or C6 have both oxidizing and reducing capabilities.[18] N1-glycosidic bond rupture was proposed to be caused by the cationic C6 lesion, arising as a result of one-electron removal of the 5,6-dihydro-6-thymyl radical,[19] whereas the capture of an additional electron by the cytosine N3−H atom radical adduct led to the automatic rupture of the C3′−O(P) bond.[20] The electron detachment energy of 5′dAMP-H anionic radicals, which results through OH radical induced H abstraction from the sugar, was calculated to explore the effects of DNA damage.[21] The work reported herein primarily refers to deoxythymidine 3′-monophosphate (3′dTMP, cf. Chart 1), which is employed to model the 3′-terminal of the DNA strand. Given the complex and asymmetric local environment, both 'back' and 'front' attacks at the C5 site of the base by OH and H radicals are considered. In particular, the processes of carbon-centered H-atom transfer from C2′ on the sugar moiety to C6 on the radical-modified thymine base are explored in detail. The bond dissociation energy (BDE) of the C3′−O(P) and C1′−N1 (glycosidic) bonds and the activation barriers are calculated in order to investigate possible cleavage modes in DNA under radical stress. In addition, the direct effects of electronic attack on the H-transfer barrier, both without and including additional H/OH radical addition to thymine, are investigated.

Chart 1

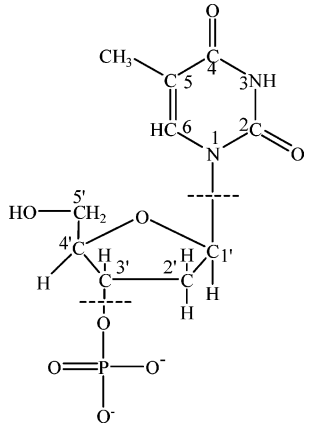

2. Methodology

All geometries were optimized at the hybrid Hartree−Fock-density functional theory B3LYP level,[22,23] in conjunction with the 6-31+G(d,p) basis set. Frequency calculations were performed at the same level of theory, to confirm the correct nature of the stationary points. From the frequency calculations, zero-point energies (ZPE) were extracted and added to the electronic energies, as applicable. Natural bond orbital (NBO) theory[24] and natural population analysis (NPA) were used to determine atomic charges. Bulk solvation effects were considered using the integral equation formalism of the polarized continuum model (IEF-PCM)[25] with dielectric constants $\epsilon = 4.3$ and $\epsilon = 78.4$, respectively, to model the extreme cases of a hydrophobic environment and of aqueous solution. Vertical electron affinities (VEA) were determined

Table 1. ZPE-Corrected Reaction Energies and Activation Barriers (in kcal/mol) for the H-Atom Transfer Reactions at the B3LYP/6-31+G(d,p) Level

reactions	TH1′→ TH3′	TH1→ TH3	TOH1′→ TOH3′	TOH1→ TOH3
transition barrier				
vacuum	23.9	25.1	21.7	24.1
$\epsilon = 4.3$	24.6	25.0	21.0	19.7
$\epsilon = 78.4$	25.3	24.2	19.0	23.1
reaction energy				
vacuum	4.6	6.3	2.3	5.8
$\epsilon = 4.3$	4.5	5.2	1.7	−6.2
$\epsilon = 78.4$	3.4	4.7	0.8	−4.8

as the energy difference of the parent compound and its reduced form, evaluated at the optimized geometry of the parent compound. Bond dissociation energies (BDE) for the fragmentation reactions were obtained by evaluating the ZPE-corrected energy difference between the optimized fragments and the complex. No basis set superposition effects (BSSE) were considered in these calculations, based on the sizes of the systems in question and the fact that such corrections can be expected to be much smaller than the evaluated energy differences to change any of the conclusions drawn from the computed data. All calculations were performed using the Gaussian 03 package.[26] Atomic labeling used in the text and tables throughout refers to Chart 1. The DNA strand was truncated by hydrogen atoms at the C5′OH and the C3′−$OP(O)_2^-$OH ends, and the phosphate was kept negatively charged to ensure an appropriate environment. The use of a negatively charged phosphate group proved to be of importance to the results obtained, as will be discussed below.

3. Results and Discussions

3.1. H Atom Transfer Initiated by H Radical or Free Electron Addition. As previously noted, H atom addition in 3′dTMP occurs primarily on the pyrimidine C5 atom. Two cases are considered herein—H atom attack from the back (‘primed’) and front (‘unprimed’) at the C5 site of the base, TH1′ and TH1, respectively (cf. Chart 1). The energy difference between the two radical adducts is 1.7 kcal mol^{-1} in favor of the ‘front’ adduct TH1, due to more favorable interaction between the phosphate group and the sugar and between the C5′OH group and the radical site. The radical centers are, as expected, localized at C6 in both cases (C6 spin densities 0.752 e in TH1 and 0.736 e in TH1′). Among the H atoms of the deoxyribose moiety, H2′ is the one closest to the radical center C6, at a distance of 2.855 Å in TH1 and 2.677 Å in TH1′. H2′ abstraction by the C6 radical center has been attributed to be responsible for strand breaks[27] and is the primary reaction studied herein.

The activation barrier for H2′ atom transfer to C6 is 23.9 kcal mol^{-1} in TH1′→TH3′; 1−2 kcal mol^{-1} lower than for the TH1→TH3 case. Since the two transition states TH2 and TH2′ have almost the same energy (see Table 1), the barrier difference is attributed to the different stability of the reactants TH1 and TH1′. In TH2′, the C2′−H2′ distance is

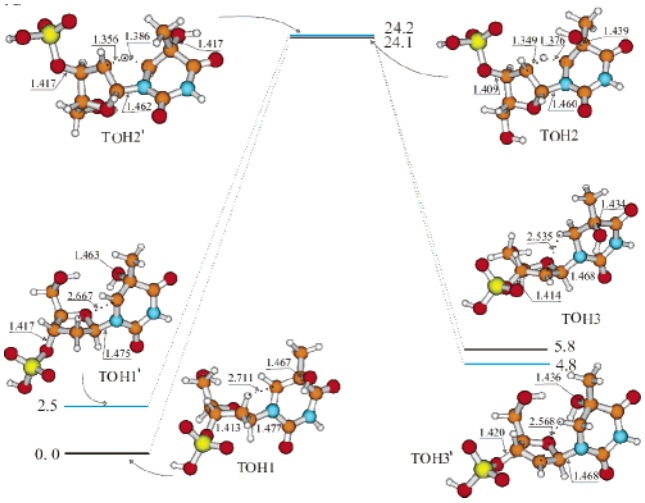

Figure 1. Energy profiles and selected geometrical parameters of the stationary structures along the H atom abstraction reaction TOH1(′)→TOH3(′), obtained at the ZPE-corrected UB3LYP/6-31+G(d,p) level.

1.355 Å, 0.03 Å shorter than H2′−C6. The spin density is mainly localized on C2′ (0.676 e), C3′ (−0.136 e), and C6 (0.532 e), clearly illustrating the spin transfer associated with these reactions. H2′ has a spin density of −0.084 e in TH2′, compared to −0.002 e in TH1′ and TH3′. The situation is highly analogous in the ‘front’ transition state TH2. The H atom transfer produces a sugar-centered radical localized on C2′, which forms a potential basis for subsequent reactions such as electron transfer, H atom transfer along the deoxyribose moiety, and/or addition of O_2. The C1′−N bond length is shortened in both TH3 and TH3′, as compared with the reactant species, whereas C3′−O(P) becomes slightly elongated.

To elucidate the influence of electron addition on the sugar-to-base H atom transfer, the H2′ abstraction reaction was also studied following the reduction of 3′dTMP, rather than addition of hydrogen or hydroxyl radicals. The unpaired spin in the 3′dTMP electronic adduct is mainly localized to C6 (0.58 e), compared with the spin density of approximately 0.74−0.75 e on C6 in TH1 and TH1′. The activation barrier in the gas phase is 29.3 kcal mol^{-1}, and the overall reaction energy is endothermic by 21.0 kcal mol^{-1}. Compared with the above H atom-induced abstraction reaction, it shows that an additional proton added to C5 is favorable for the reaction by reducing the barrier by ∼4 kcal mol^{-1} and contributes to a drastic lowering of the reaction energy, from 21.0 to 6.3 kcal mol^{-1}. The results emphasize the fact that the local field can play an important role on mediating these reactions.

3.2. H Atom Transfer Initiated by OH Radical Addition. In analogy with the C5−H adducts described above, the role of hydroxyl radical addition to C5 on C6−H2′ abstraction was investigated. The C5−O(H), N1−C1′, and C3′−O(P) bond lengths are essentially identical in the two cases (‘front’ adduct TOH1 and ‘back’ adduct TOH1′, respectively), as are the C6···H2′ distances (cf. Figure 1). As shown in Figure 1, TOH1′ is less stable than TOH1 by 2.5 kcal mol^{-1}, which can be correlated to a slightly weaker

repulsion between the thymine-OH group and the sugar moiety in TOH1.

The gas-phase activation barrier for H2′ atom transfer to C6 is 21.7 kcal mol^{-1} for TOH1′→TOH3′, which is 2.6 kcal mol^{-1} lower than in the TOH1→TOH3 case. The distances between H2′ and C2′ (C6) are 1.356 (1.386) Å, respectively, in TOH2′ and slightly shorter in TOH2. The N1−C1′ bond length is shortened somewhat during the H atom transfer, although the N1−C1′ and C3′−O(P) bond differences when going from reactant to product are smaller in the case of the C5−OH adducts compared to the above C5−H systems. The reaction energy is endothermic by 2.3 kcal mol^{-1} for TOH1′→TOH3′ and 5.8 kcal mol^{-1} for TOH1→TOH3. The spin transfer from C6 in TOH1 and TOH1′, to the radical center localized on C2′ in TOH3 and TOH3′, is very similar to the H-adduct cases.

3.3. Effects of Bulk Solvation on the Reactive Profiles. The role of bulk solvation on the reaction profiles was explored through the use of a surrounding dielectric medium with $\epsilon = 4.3$ and 78.4 to simulate extreme cases in the local surroundings of DNA. In Table 1, the energetics derived from the density functional theory self-consistent reaction field (DFT-SCRF) calculations are listed. Several features can be observed from the reaction profiles after accounting for the implicit solvent effects generated by the nonaqueous and aqueous medium. First of all, the barriers for the TH1′→TH3′ and TH1→TH3 reactions are nearly unchanged, showing that bulk solvation does not influence the reaction rates. For the TOH1′→TOH3′ reaction, the barrier is lowered to 19.0 kcal mol^{-1} in aqueous medium. Almost the same barrier height is found for TOH1→TOH3 reaction in the nonaqueous medium.

Regarding the overall reaction energies, bulk solvation effects throughout contribute favorably to the H atom transfer. The OH radical-induced reactions are preferred over H radical-induced ones by up to 10 kcal mol^{-1}. In aqueous medium, the reaction energy of TOH1′→TOH3′ is essentially thermoneutral, whereas the bulk solvation effects are even more favorable to the TOH1→TOH3 reaction; these now become exothermic by 4.8 kcal mol^{-1} in aqueous medium and 6.2 kcal mol^{-1} in the nonaqueous medium. Thus, the H atom transfer reaction is strongly dependent on radical species, direction of attack ('back' or 'front' of base plane), and surrounding medium.

In addition, the radical intermediates have very diverse properties.[18] Depending on the local surroundings, the species can capture one electron and become closed-shell dianions (the phosphate groups already carry a negative charge) or donate an electron to a suitable acceptor. For the possibility of the former, Gutowski et al. considered anionic resonance states as a path to valence bound anionic states.[20] The electron affinities of separate DNA bases are well characterized and understood.[28] Herein, we have calculated the vertical electron affinities (VEA) of the OH− or H−3′dTMP anion radicals, within the present theoretical level. According to the data given in Table 2, the gas-phase VEAs are consistently negative, showing that the closed-shell dianion species become unstable in the gas phase. Bulk solvation already at $\epsilon = 4.3$ contributes to the stability of the dianion and renders all the VEAs positive. In addition, in solution the reactant VEAs are always greater than those of the products.

Table 2. Vertical Electron Affinities (in eV)

	TH1′	TH1	TH3′	TH3
vacuum	−1.6	−1.7	−2.1	−2.1
$\epsilon = 4.3$	1.3	1.3	1.2	1.2
	TOH1′	**TOH1**	**TOH3′**	**TOH3**
vacuum	−1.0	−1.1	−2.0	−2.0
$\epsilon = 4.3$	2.0	2.1	1.3	1.0

NBO charges are calculated on the different products as well as their corresponding closed-shell electron adduct species in vacuum and nonaqueous solution (ϵ=4.3). The results are listed in Table 3. For the radical adducts, which are anionic due to the unprotonated oxygen in the phosphate groups, the negative charges are mainly localized on the phosphate (−1.22 e$^-$) and radical-modified thymine (−0.260 to −0.278 e$^-$). The sugar groups carry a positive charge (0.479−0.499 e$^-$). Upon the capture of an excess electron, the negative charge on the phosphate groups remains essentially unaltered (−1.31 e$^-$), whereas for the modified thymine, the negative charge is increased to up to −0.534 e$^-$. The most significant changes are assigned to the sugar groups, where the negative charge increases by about 0.67 e$^-$. The captured electron will hence mainly be localized to the sugar group. Bulk solvation tends to move the negative charge in the electron adduct from the base to the sugar but does not effect the charge on the phosphate.

Another interesting result is that the N1-glycosidic bond automatically decomposes upon reduction. In, for example, the closed-shell TH3 anion adduct, NBO charge analysis shows that the altered base behaves as the leaving group with −0.936 e$^-$ charge, a slight positive charge is found on the sugar, and a nearly unchanged negative charge (−1.3 e$^-$) remains on the phosphate. The data show that ∼0.4 e$^-$ are transferred from the sugar to the altered base upon the N1-glycosidic bond breakage. The data differ from the findings of Gutowski et al.,[20] where instead the C3′−O(P) bond is ruptured. The reason for this discrepancy is the fact that Gutowski employed a neutral (protonated) phosphate, which hence allows this group to function as an unphysical electron sink. The importance of using negatively charged phosphates in the determination of sugar C′−H bond dissociation energies has recently been emphasized in a very careful study by Guo and co-workers.[29] It was very clearly shown, that using neutral (protonated) phosphates gave a much different ordering in relative C′−H bond strengths of the sugar moiety, as compared to the results when anionic phosphates were employed. As opposed to the former, the latter systems were able to account fully for the experimental findings for these systems. In the current model, we note that the charged phosphate leads to a repulsive effect between the negative charges and spontaneous base release.

The energetics are markedly different from that seen in the corresponding 5′dTMP model, previously investigated in our group.[30] In that case, the barriers to H transfer were 5−10 kcal/mol higher for the different anionic radical

Table 3. NPA Charge Distribution on Base (B), Sugar (S), and Phosphate Group (P) of the Radical Anions and Their Vertical and Adiabatic Closed-Shell Electron Adducts in Vacuum and in Nonaqueous Solution (in Parentheses)

	radical anion			electron adduct[a]			electron adduct[b]		
	B	S	P	B	S	P	B	S	P
TH3′	−0.26	0.48	−1.22	−0.53	−0.18	−1.29	−0.94	0.22	−1.28
				(−0.39)	(−0.30)	(−1.31)	(−0.93)	(0.23)	(−1.30)
TH3	−0.26	0.48	−1.22	−0.51	−0.19	−1.29	−0.94	0.22	−1.28
				(−0.38)	(−0.30)	(−1.32)	(−0.93)	(0.23)	(−1.30)
TOH3′	−0.28	0.50	−1.22	−0.53	−0.17	−1.30	−0.94	0.22	−1.28
				(−0.41)	(−0.27)	(−1.32)	(−0.94)	(0.23)	(−1.30)
TOH3	−0.26	0.48	−1.22	−0.51	−0.21	−1.29	−0.95	0.23	−1.28
				(−0.38)	(−0.31)	(−1.31)	(−0.94)	(0.24)	(−1.30)

[a] Vertical electron addition to radical anion. [b] Adiabatic species, leading to spontaneous base release.

adducts; the lowest barrier was there obtained for the TH1→TH3 system, at 27.0 kcal mol^{-1}. Upon addition of an excess electron to those system, spontaneous base release did not occur, but a drastic reduction in H transfer barrier was observed, especially for the H radical adducts (to between 5 and 15 kcal mol^{-1}). Subsequent to H transfer, the barrier to C1′−N1 bond rupture was only a few kcal mol^{-1}. Base release will, hence, eventually be the observed lesion also in the reduced radical adducts, although the 5′dTMP systems appear to be considerably less reactive than the current 3′dTMP ones. This can be understood from the closer proximity to the lesion in 3′dTMP than in 5′dTMP.

3.4. Free Radical Induced Bond Scission. Upon the formation of the C2′-centered radical (i.e., without the additional reduction), the unpaired electron can be transferred to the neighboring atoms, C1′ and C3′. The C−C bond lengths on the sugar moiety provide some indications for this. For example, the C1′−C2′ and C2′−C3′ bond lengths are respectively 1.529 and 1.543 Å in TH1′. After H2′ is transferred to the C6 site of the base, the two bonds become shorter and of equal lengths. Delocalization of the unpaired electron to the neighboring carbon atoms hence occur, which in turn influence N1−C1′ or C3′−O(P) bond dissociation. It is thus of interest to explore the thermodynamic properties of potential bond dissociation induced by the radical adduct formation. In this section, we discuss bond dissociation energies (BDE) toward strand scission and base release, presented in Table 4.

Homolytic dissociation of the N1-glycosidic bond leading to the formation of a neutral base (B) radical and a negatively charged closed shell sugar−phosphate (SP) moiety was found to be highly favored over heterolysis, with BDE values ranging from 29.1 to 32.2 kcal mol^{-1} in gas phase. Both homolytic and heterolytic base release leads to the formation of a C1′═C2′ double bond in the sugar ring. Bulk solvation (ϵ=4.3) contributes to a lowering of the homolytic BDE by 2−8 kcal mol^{-1}. Even larger effects are noted for the heterolytic process, due to the negatively charged base formed. The BDE values of TH3′ and TH3 are lower than those of TOH3′ and TOH3 for the homolytic process but larger in the case of heterolysis.

Rupture of C3′−O(P) is also explored and can be compared to the dissociation of the N1-glycosidic bond; again both homolysis and heterolysis are calculated, the latter

Table 4. ZPE-Corrected Gas-Phase Bond Dissociation Energies (in kcal mol^{-1}) for Base Release or Strand Break[d]

N1−C1′	TH3′	TH3	TOH3′	TOH3
homolysis	29.1	29.1	32.2	31.1
	(22.2)	(22.7)	(24.0)	(29.2)
heterolysis[a]	55.5	55.5	51.3	50.2
	(45.5)	(45.9)	(42.6)	(47.8)
heterolysis[b]	335.8	335.8	255.4	254.4
	(217.3)	(217.7)	(142.3)	(147.5)
C3′−O(P)	TH3′	TH3	TOH3′	TOH3
homolysis	19.1	19.3	18.1	20.0
	(9.4)	(10.1)	(8.6)	(15.2)
heterolysis[c]	262.0	259.7	261.8	265.4
	(97.9)	(97.4)	(101.2)	(104.5)

[a] Base (B) is closed-shell anion; sugar−phosphate (SP) moiety neutral doublet. [b] B is closed-shell cation; SP doublet dianion. [c] SB is neutral doublet; P singlet dianion. [d] Values in nonaqueous medium (ϵ=4.3) given in parentheses.

associated with HPO_4^{2-} as the leaving group. Also in this case homolytic dissociation is favored, with BDE values ranging from 18.1 to 20.0 kcal mol^{-1}, whereas the heterolytic processes require far more energy. Bulk solvation plays a significant role in reducing the BDE values, by 5−10 kcal mol^{-1} for homolytic dissociation and around 160.0 kcal mol^{-1} for heterolysis (due to the dianionic phosphate formed).

From the computed data, it is clear that homolytic dissociation is the primary reaction under H and OH radical stress and that cleavage of C3′−O(P) is dominant over that of the N1-glycosidic bond, assuming that the systems are not influenced by additional electron capture. Further implications are given by the structural changes. The N1−C1′ bond lengths are all contracted, whereas the C3′−O(P) ones become slightly longer during the TH1(′) → TH3(′) and TOH1(′) → TOH3(′) reactions, which also indicates that cleavage of C3′−O(P) is expected to be the dominant process over N1-glycosidic bond rupture upon radical formation.

In order to obtain a reliable bond scission profile in vacuum, the potential energetic surface (PES) was scanned from TOH3′ to the decomposed species by varying C3′⋯O(P) and C1′⋯N1 distances with a step-length of 0.1 Å, respectively, and optimizing the remaining coordinates. The energies for the C3′O(P) and C1′N1 bonds scans are

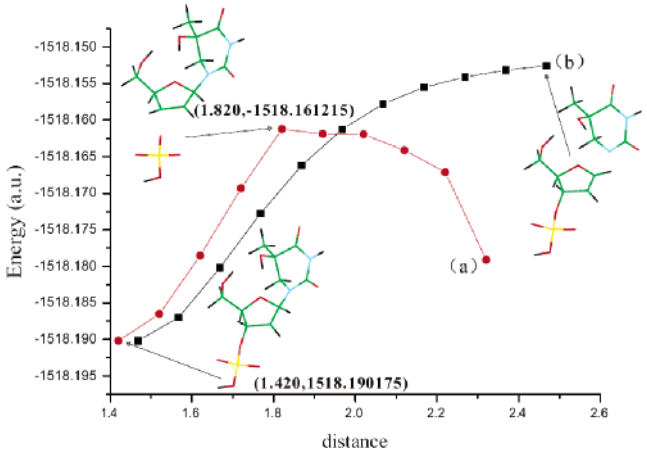

Figure 2. The decomposition curves for the C3′−O(P) and C1′−N1 bonds of TOH3′, obtained at the B3LYP/6-31+G-(d,p) level (without ZPE corrections): (a) the C3′−O(P) bond dissociation and (b) the C1′−N1 bond dissociation.

displayed in Figure 2. For the C3′O(P) bond PES, there is a quasi-saddle point at the C3′···O(P) distance of 1.820 Å with an energy at the B3LYP/6-31+G(d,p) level of approximately 18.2 kcal mol^{-1} relative to the TOH3′ starting point, comparable to the value needed for the decomposition of the N1-glycosidic bond of the dT electron adduct[31] and less than the energy required for the initial C2′−H transfer. For the elongation of the C1′−N1 bond, the energy is continuously increasing during the 1.0 Å increase in bond length. The results show that the C3′−O(P) bond is facile to be decomposed, while the N1-glycosidic bond remains stable under radical stress, which is consistent with the BDE calculations.

In a very recent paper, the heterolytic process of the N9-glycosidic bond cleavage in 2′-deoxyguanosine promoted by cations, especially by dicationic systems, was reported.[32] The BDE values obtained were 44.3 (singly protonated), 58.0 (Cu^{+}), −29.2 (Cu^{2+}), and −36.2 (doubly protonated) kcal mol^{-1}, respectively. All results taken together illustrate that the decomposition modes are strongly dependent on the local DNA environment (electron attachment, proton transfer, metal ion or radical stress) and on the stability of the decomposed species. We also emphasize again that the usage of appropriately charged models appears to be essential.

4. Conclusions

In the present work, hybrid DFT methods have been employed to investigate the potential DNA-scission processes induced by H and OH radical addition to the C5 site of thymine in 3′dTMP. Geometries, unpaired electron spin densities, NPA charges, and reaction energies were obtained at the B3LYP/6-31+G(d,p) level in the gas phase, followed by energy calculations performed at the same level in solution (ϵ=4.3 and 78.4) using IEF-PCM to model bulk solvation. The barriers of subsequent C2′−H abstraction by the C6 radical site range from 21.7 to 25.1 kcal mol^{-1} in the gas phase and 19.0 to 25.3 kcal mol^{-1} in aqueous solution. Bulk solvation contributes more markedly by reducing the reaction energies, especially for the OH radical adducts.

Vertical electron affinities were determined and showed that the capture of an excess electron by the radical systems is favored by solvation also in nonaqueous medium. NPA charges show that the negative charges of the radical adducts are situated on the radical-modified base and the phosphate fragments, respectively. Addition of an excess electron has significant consequences to the system. The additional electron is initially localized on the sugar fragment. However, all electron adducts were found to result in base release upon structural relaxation, with concomitant transfer of the added electron to be entirely localized on the leaving base.

Analysis of bond dissociation energies (BDE) of the N1−C1′ (N1-glycosidic bond) and C3′−O(P) bonds of the radical products TH3(′) and TOH3(′) were performed. A homolytic process is supported for both cases and C3′−O(P) bond rupture seems more favorable than the rupture of the N1-glycosidic bond. The C3′−O(P) bond is facile to be decomposed with a barrier of 18.2 kcal mol^{-1}, while the N1-glycosidic bond is still stable under the radical stress. The change in N1−C1′ and C3′−O(P) bond lengths before and after the reactions support the above conclusion. The nonaqueous bulk solvation contributes to the bond rupture through a drastic decrease of the homolytic BDE value by up to 15 kcal mol^{-1}.

Acknowledgment. The Swedish Science Research Council (VR) and the National Natural Science Foundation of China (Grant No. 20643007) are gratefully acknowledged for financial support. We also acknowledge generous grants of computing time at the National supercomputing facilities in Linköping (NSC).

References

(1) von Sonntag, C.; Schuchman, H.-P. Ionizing radiation damage to DNA. In *Encyclopedia of Molecular Biology and Molecular Medicine*; Meyers, R. A., Ed.; VCH Weinheim: 1996; Vol. 3, pp 354−365.

(2) Halliwell, B.; Gutteridge, J. M. C. *Free Radicals in Biology and Medicine*; Oxford University Press: Oxford, U.K., 1999.

(3) Stein, G.; Weiss, J. Chemical effects of ionizing radiations. *Nature* **1948**, *161*, 650.

(4) Commoner, B.; Townsend, J.; Pake, G. E. Free Radicals in Biological Materials. *Nature* **1954**, *174*, 689.

(5) Nauser, T.; Schöneich, C. Thiyl Radical Reaction with Thymine: Absolute Rate Constant for Hydrogen Abstraction and Comparison to Benzylic C-H Bonds. *Chem. Res. Toxicol.* **2003**, *16*, 1056.

(6) Ramírez-Arizmendi, L. E.; Heidbrink, J. L.; Guler, L. P.; Kenttämaa, H. I. Reactivity of Substituted Charged Phenyl Radicals toward Components of Nucleic Acids. *J. Am. Chem. Soc.* **2003**, *125*, 2272.

(7) von Sonntag, C. *The Chemical Basis of Radiation Biology*; Taylor & Francis: London, U.K., 1987.

(8) Wetmore, S. D.; Boyd, R. J.; Eriksson, L. A. Theoretical Investigation of Adenine Radicals Generated in Irradiated DNA Components. *J. Phys. Chem. B* **1998**, *102*, 10602.

(9) Drew, H. R.; Wing, R. M.; Takano, T.; Broka, C.; Tanaka, S.; Itakura, K.; Dickerson, R. E. Structure of a B-DNA Dodecamer: Conformation and Dynamics. *Proc. Natl. Acad. Sci. U.S.A.* **1981**, *78*, 2179.

(10) Balasubramanian, B.; Pogozelski, W. K.; Tullius, T. D. Failure of egg cylinder elongation and mesoderm induction in mouse embryos lacking the tumor suppressor smad2. *Proc. Natl. Acad. Sci. U.S.A.* **1998**, *95*, 9738.

(11) Lemaire, D. G. E.; Bothe, E.; Schulte-Frohlinde, D. Yields of Radiation-induced Main Chain Scission of Poly U in Aqueous Solution: Strand Break Formation Via Base Radicals. *Int. J. Radiat. Biol*. **1984**, *45*, 351.

(12) Symons, M. C. R. Application of electron spin resonance spectroscopy to the study of the effects of ionising radiation on DNA and DNA complexes. *J. Chem. Soc., Faraday Trans*. **1987**, *83*, 1.

(13) Becker, D.; Sevilla, M. D. In *Advances in Radiation Biology, Volume 17, DNA and Chromatin Damage Caused by Radiation*; Lett, J. T., Sinclair, W. K., Eds.; Academic Press: New York, 1987.

(14) Bothe, E.; Qureshi, G. A.; Schulte-Frohlinde, D. Rate of OH radical induced strand break formation in single stranded DNA under anoxic conditions. An investigation in aqueous solutions using conductivity methods. *Z. Naturforsch*. **1983**, *38C*, 1030.

(15) (a) Karam, L. R.; Dizdaroglu, M.; Simic, M. G. Intramolecular H Atom Abstraction from the Sugar Moiety by Thymine Radicals in Oligo- and Polydeoxynucleotides. *Radiat. Res*. **1988**, *116*, 210. (b) Deeble, D. J.; von Sonntag, C. Radiolysis of Poly(U) in Aqueous Solution. The Role of Primary Sugar and Base Radicals in the Release of Undamaged Uracil. *Int. J. Radiat. Biol*. **1984**, *46*, 247.

(16) (a) Hildenbrand, K.; Behrens, G.; Schulte-Frohlinde, D.; Herak, J. N. Comparison of the reaction of OH and of $SO4^{-}$ radicals with pyrimidine nucleosides. An electron spin resonance study in aqueous solution. *J. Chem.* Soc., *Perkin Trans. 2* **1989**, 283. (b) Schulte-Frohlinde, D.; Hildenbrand, K. In *Free Radicals in Synthesis and Biology;* Minisci, F., Ed.; 1989; p 335. (c) Schulte-Frohlinde, D.; Opitz, J.; Gomer H.; Bothe, E. Model studies for the direct effect of high-energy irradiation on DNA. Mechanism of strand break formation induced by laser photoionization of poly U in aqueous solution. *Int. J. Radiat. Biol*. **1985**, *48*, 397. (d) Wagner, J. R.; van Lier, J. E.; Johnston, L. J. Quinone sensitized electron transfer photooxidation of nucleic acids: chemistry of thymine and thymidine radical cations in aqueous solution. *Photochem. Phorobiol*. **1990**, *52*, 333. (e) Krishna, C. M.; Decarroz, C.; Wagner, J. R.; Cadet J.; Riesz, P. Menadione sensitized photooxidation of nucleic acid and protein constituents. An ESR and spin-trapping study. *Photochem. Photobiol*. **1987**, *46*, 175.

(17) Barvian, M. R.; Barkley, R. M.; Greenberg, M. M. Reactivity of 5,6-Dihydro-5-hydroxythy- mid -6-yl Generated via Photoinduced Single Electron Transfer and the Role of Cyclohexa-1,4-diene in the Photodeoxygenation Process. *J. Am. Chem. Soc*. **1995**, *117*, 4894.

(18) Colson, A.-O.; Sevilla, M. D. Ab Initio Molecular Orbital Calculations of Radicals Formed by H• and •OH Addition to the DNA Bases: Electron Affinities and Ionization Potentials. *J. Phys. Chem*. **1995**, *99*, 13033.

(19) Zhang, Q.; Wang, Y. Independent Generation of the 5-Hydroxy-5,6-dihydrothymidin-6-yl Radical and Its Reactivity in Dinucleoside Monophosphates. *J. Am. Chem. Soc*. **2004**, *126*, 13287.

(20) Dabkowska, I.; Rak, J.; Gutowski, M. DNA strand breaks induced by concerted interaction of H radicals and low-energy electrons-A computational study on the nucleotide of cytosine. *Eur. Phys. J. D* **2005**, *35*, 429.

(21) Hou, R.; Gu, J.; Xie, Y.; Yi, X.; Schaefer, H. F., III. The 2′-Deoxyadenosine-5′- phosphate Anion, the Analogous Radical, and the Different Hydrogen-Abstracted Radical Anions: Molecular Structures and Effects on DNA Damage. *J. Phys. Chem. B* **2005**, *109*, 22053.

(22) Becke, A. D. Density-functional thermochemistry. III. The role of exact exchange. *J. Chem. Phys*. **1993**, *98*, 5648.

(23) Lee, C.; Yang, W.; Parr, R. G. Development of the Colle-Salvetti correlation-energy formula into a functional of the electron density. *Phys. Rev. B* **1988**, *37*, 785.

(24) Reed, A. E.; Curtiss, L. A.; Weinhold, F. Intermolecular interactions from a natural bond orbital, donor-acceptor viewpoint. *Chem. Rev*. **1988**, *88*, 899.

(25) Tomasi, J.; Persico, M. Molecular Interactions in Solution: An Overview of Methods Based on Continuous Distributions of the Solvent. *Chem. Rev*. **1994**, *94*, 2027.

(26) Frisch, M. J.; Trucks, G. W.; Schlegel, H. B.; Scuseria, G. E.; Robb, M. A.; Cheeseman, J. R.; Montgomery, J. A., Jr.; Vreven, T.; Kudin, K. N.; Burant, J. C.; Millam, J. M.; Iyengar, S. S.; Tomasi, J.; Barone, V.; Mennucci, B.; Cossi, M.; Scalmani, G.; Rega, N.; Petersson, G. A.; Nakatsuji, H.; Hada, M.; Ehara, M.; Toyota, K.; Fukuda, R.; Hasegawa, J.; Ishida, M; Nakajima,. T.; Honda, Y.; Kitao, O.; Nakai, H.; Klene, M.; Li, X.; Knox, J. E.; Hratchian, H. P.; Cross, J. B.; Adamo, C.; Jaramillo, J.; Gomperts, R.; Stratmann, R. E.; Yazyev, O.; Austin, A. J.; Cammi, R.; Pomelli, C.; Ochterski, J. W.; Ayala, P. Y.; Morokuma, K.; Voth, G. A.; Salvador, P.; Dannenberg, J. J.; Zakrzewski, V. G.; Dapprich, S.; Daniels, A. D.; Strain, M. C.; Farkas, O.; Malick, D. K.; Rabuck, A. D.; Raghavachari, K.; Foresman, J. B.; Ortiz, J. V.; Cui, Q.; Baboul, A. G.; Clifford, S;. Cioslowski, J.; Stefanov, B. B.; Liu, G.; Liashenko, A.; Piskorz, P.; Komaromi, I.; Martin, R. L.; Fox, D. J.; Keith, T.; Al-Laham, M. A.; Peng, C. Y.; Nanayakkara, A.; Challacombe, M.; Gill, P. M. W.; Johnson, B.; Chen, W.; Wong, M. W.; Gonzalez, C.; Pople, J. A. *Gaussian 03, Revision B.04*; Gaussian, Inc.: Pittsburgh, PA, 2003.

(27) Pardo, L.; Banfelder, J. T.; Osman, R. Ab initio LCAO-MO-SCF study of bonding in the simplest phosphorus ylide. *J. Am. Chem. Soc*. **1992**, *114*, 2382.

(28) (a) Oyler, N. A.; Adamowicz, L. Electron attachment to uracil: theoretical ab initio study. *J. Phys. Chem*. **1993**, *97*, 11122. (b) Hendricks, J. H.; Lyapustina, S. A.; de Clercq, H. L.; Bowen, K. H. The dipole bound-to-covalent anion transformation in uracil. *J. Chem. Phys*. **1998**, *108*, 8. (c) Wetmore, S. D.; Boyd, R. J.; Eriksson, L. A. Electron affinities and ionization potentials of nucleotide bases. *Chem. Phys. Lett*. **2000**, *322*, 129. (d) Wesolowski, S. S.; Leininger, M. L.; Pentchev, P. N.; Schaefer, H. F., III. Electron Affinities of the DNA and RNA Bases. *J. Am. Chem. Soc*. **2001**, *123*, 4023.

(29) Li, M.-J.; Liu, L.; Wei, K.; Fu, Y.; Guo, Q.-X. Significant Effects of Phosphorylation on Relative Stabilities of DNA and RNA Sugar Radicals: Remarkably High Susceptibility of H-2′ Abstraction in RNA. *J. Phys. Chem. B* **2006**, *110*, 13582.

(30) Zhang, R. B.; Eriksson, L. A. The Role of Nucleobase Carboradical and Carbanion on DNA Lesions: A Theoretical Study. *J. Phys. Chem. B* **2006**, *110*, 23583.

(31) Gu, J.; Xie, Y.; Schaefer, H. F., III. Glycosidic Bond Cleavage of Pyrimidine Nucleosides by Low-Energy Electrons: A Theoretical Rationale. *J. Am. Chem. Soc*. **2005**, *127*, 1053.

(32) Ríos-Font, R.; Bertrán, J.; Rodríguez-Santiago, L.; Sodupe, M. Effects of Ionization, Metal Cationization and Protonation on 2′-Deoxyguanosine: Changes on Sugar Puckering and Stability of the N-Glycosidic Bond. *J. Phys. Chem. B* **2006**, *110*, 5767.

CT6003593